Stabilization of the Less Common $(d_{xz}d_{yz})^4(d_{xy})^1$ Iron(III) Porphyrin Ground Electronic State: ^{1}H NMR Investigations of Iron(III) 5,10,15,20-Tetracyclohexylporphyrin

Stanisław Wołowiec, Lechosław Latos-Grażyński,* Dawn Toronto, and Jean-Claude Marchon*

Department of Chemistry, University of Wrocław, 14 F. Joliot-Curie St., Wrocław 50 383, Poland, and Département de Recherche Fondamentale sur la Matiére Condensée, SCIB/Laboratoire de Chimie de Coordination, CEA Grenoble, F-38054 Grenoble, France

Received June 27, 1997

High-spin and low-spin complexes of the iron(III) tetrakis(*meso*-cyclohexyl)porphyrin ((TCHP)Fe^{III}) have been studied by means of 1-D and 2-D ^{1}H NMR. The complete assignment of porphyrin and R-imidazole ^{1}H resonances has been done on the basis of 2-D COSY and NOESY techniques as well as by selective deuteration of imidazole. The chemical shifts of pyrrole β-Hs have been used as the probe of the electronic state of an iron(III) metal ion. It has been found that cyanide coordinates to the high-spin (TCHP)Fe^{III}Cl complex, leading to the formation of the low-spin $[(TCHP)Fe^{III}(CN)_2]^-$, with the rare $(d_{xz}d_{yz})^4(d_{xy})^1$ ground electronic state (the pyrrole β-H resonance at 12.01 ppm at 293 K in CD_3OD). A contribution of two electronic configurations, $(d_{xy})^2(d_{xz}d_{yz})^3$ and $(d_{xz}d_{yz})^4(d_{xy})^1$, to the ground state of the metal ion has been invoked for the low-spin $[(TCHP)Fe^{III}(R\text{-}Im)_2]^+$ complexes. Characteristic ^{1}H NMR shifts for these complexes include the pyrrole resonance at 2.81 ppm accompanied by the markedly upfield shifted imidazole resonances at −19.67 ppm (2-H), −10.58 ppm (4-H), −4.05 ppm (5-H), and 0.97 ppm (1-H). An admixture of a $(d_{xz}d_{yz})^4(d_{xy})^1$ configuration into the ground electronic state increases in the order imidazole (ImH) < 1-methylimidazole (1-MeIm) < 1,2-dimethylimidazole (1,2-diMeIm), following an enlargement of the axial ligand steric hindrance. The rotation of the 1,2-diMeIm around Fe−N bond in the low-spin $[(TCHP)Fe^{III}(1,2\text{-}diMeIm)_2]^+$ complex is slow on the ^{1}H NMR time scale even at 293 K. Consequently four β-H resonances and the diastereotopy of the cyclohexyl *meso*-substituents have been observed. The *meso*-cyclohexyl groups rotate freely at temperature above 243 K, whereas the frozen rotation below 233 K leads to the formation of additional rotational isomers as demonstrated by multiplicity of β-H resonances for high-spin and low-spin complexes studied.

Introduction

Replacement of *meso*-aryl substituents of widely investigated metallotetrarylporphyrin by alkyl groups may profoundly influence the molecular and electronic structure as well as catalytic properties of the resulting complexes. Sterically demanding groups at the porphyrin periphery generally introduce an extensive nonplanar distortion of the relatively flexible porphyrin macrocycle.[1−4] Conformationally constrained porphyrins and metalloporphyrins have been proposed as model systems to study the electronic consequences of ring deformations.[5,6]

The conformational flexibility of the porphyrin macrocycle has been considered as means of control the redox, spectroscopic and catalytic properties of metalloenzymes or metalloporphyrins[5−11] and can be involved in a control of the electronic structure of low-spin iron(III) porphyrins. Typically the ground electronic state of low-spin iron porphyrins evolves between two extreme cases, i.e., $(d_{xy})^2(d_{xz}d_{yz})^3$ and $(d_{xz}d_{yz})^4(d_{xy})^1$.[12−17] A large variety of axial ligands have been probed in order to

* To whom correspondence should be addressed: L.L.-G., University of Wrocław; J.-C.M., CEA Grenoble.

(1) Abbreviations used: P, porphyrin dianion; TPP, 5,10,15,20-tetraphenylporphyrin dianion; OEP, octaethylporphyrin dianion; TAP, 5,10,15,20-tetraisopropylporphyrin dianion; TMCP, chiroporphyrin dianion; TCHP, tetracyclohexylporphyrin dianion.

(2) (a) Barkigia, K. M.; Berber, M. D.; Fajer, J.; Medforth, C. J.; Renner, M. W.; Smith, K. M. *J. Am. Chem. Soc.* **1990**, *112*, 8851. (b) Medforth, C. J.; Senge, M. O.; Smith, K. M.; Sparks, L. D.; Shelnutt, J. A. *J. Am. Chem. Soc.* **1992**, *114*, 9859. (c) Senge, M. O.; Medforth, C. J.; Sparks, L. D.; Shelnutt, J. A.; Smith, K. M. *Inorg. Chem.* **1993**, *32*, 1716. (d) Ema, T.; Senge, M. O.; Nelson, N. Y.; Ogoshi, H.; Smith, K. M. *Angew. Chem., Int. Ed. Engl.* **1994**, *33*, 1879. (e) Jentzen, W.; Simpson, M. C.; Hobbs, J. D.; Song, X.; Ema, T.; Nelson, N. Y.; Medforth, C J.; Smith, K. M.; Veyrat, M.; Mazzanti, M.; Ramasseul, R.; Marchon, J.-C.; Takeuchi, T.; Goddard, W. A., III; Shelnutt, J. A. *J. Am. Chem. Soc.* **1995**, *117*, 11085.

(3) (a) Mandon, D.; Ochsenbein, P.; Fischer, J.; Weiss, R.; Jayaray, K.; Austin, R. N.; Gold, A.; White, P. S.; Brigaud, O.; Battioni, P.; Mansuy D. *Inorg. Chem.* **1992**, *31*, 2044. (b) Takeda, J.; Sato, M. *Tetrahedron Lett.* **1994**, *35*, 3565.

(4) (a) DiMagno, S. G.; Wersching, A. K.; Ross, I. C. R. *J. Am. Chem. Soc.* **1995**, *117*, 8279. (b) Sibilia, S. A.; Hu, S.; Piffat, C.; Melamed, D.; Spiro, T. G. *Inorg. Chem.* **1997**, *36*, 1013.

(5) Barkigia, K. M.; Chantranupong, L.; Smith, K. M.; Fajer, J. *J. Am. Chem. Soc.* **1988**, *110*, 7566.

(6) Cheng, R.-J.; Chen, P.-Y.; Gau, P.-R.; Chen, C.-C.; Peng, S.-M. *J. Am. Chem. Soc.* **1997**, *119*, 2563.

(7) Eschenmoser, A. *Ann. N.Y. Acad. Sci.* **1986**, *471*, 108.

(8) Geno, M.; Halpern, J. *J. Am. Chem. Soc.* **1987**, *109*, 1238.

(9) Plato, M.; Möbius, K.; Michele-Beyerle, M. E.; Bixon, M. E.; Jortner, J. *J. Am. Chem. Soc.* **1988**, *110*, 7279.

(10) Tsuchiya, S. *J. Chem. Soc., Chem. Commun.* **1991**, 716.

(11) Ochsenbein, P.; Mandon, D.; Fischer, J.; Weiss, R.; Austin, R. N.; Jayaray, K.; Gold, A.; Terner, J.; Bill, E.; Muether, M.; Trautwein, A. X. *Angew. Chem., Int. Ed. Engl.* **1993**, *32*, 1437.

(12) Dugad, L. B.; Medhi, O. K.; Mitra, S. *Inorg. Chem.* **1987**, *26*, 1741.

(13) Scheidt, W. R.; Geiger, D. K.; Lee, Y. J.; Reed, C. A., Lang, G. *Inorg. Chem.* **1987**, *26*, 1039.

(14) (a) Safo, M. K.; Walker, F. A.; Raitsimiring, A. M.; Walters, W. P.; Dolata, D. P.; Debrunner, P. G.; Scheidt, W. R. *J. Am. Chem. Soc.* **1994**, *116*, 7760. (b) Cheesman, M.; Walker, F. A. **1996**, *118*, 7373. (c) Walker, F. A.; Nasri, H.; Turowska-Tyrk, I.; Mohanrao, K.; Watson, C. T.; Shokhirev, N. V.; Debrunner, P. G.; Scheidt, W. R. *J. Am. Chem. Soc.* **1996**, *118*, 12109.

S0020-1669(97)00792-1 CCC: $15.00
Published on Web 02/23/1998

elucidate the relation between the ligation and the fine details of the electronic structure.[18,19] In the tetrarylporphyrin series the rare $(d_{xz}d_{yz})^4(d_{xy})^1$ ground electronic state has been stabilized by ligands which are both weak σ-donors and strong π-acceptors such as *t*-BuNC, 4-CN-Py, and P(OMe)$_2$Ph.[14−16] On the basis of EPR studies, the analogous ground electronic state was assigned to low-spin iron(III) chlorins for any low-spin type ligand.[14b,20] Recently we have demonstrated that the controlled modification of the tetrarylporphyrin periphery by addition of a quinoxaline fragment results in stabilization of the low-spin iron(III) $(d_{xz}d_{yz})^4(d_{xy})^1$ ground electronic state, even in the presence of the axial cyanide ligand.[21]

In their extensive studies on low-spin bis(substituted pyridine)iron(III) tetrarylporphyrins, Walker, Scheidt, and coworkers[14,18] have demonstrated that the stabilization of the $(d_{xz}d_{yz})^4(d_{xy})^1$ electronic state is related to a relative perpendicular orientation of two planar axial ligands along with an extensively S_4-ruffled porphyrin core. Recently Nakamura et al. have demonstrated that bis(cyano)iron(III) *meso*-tetraisopropylporphyrin reveals the $(d_{xz}d_{yz})^4(d_{xy})^1$ ground electronic state.[17a] In addition it has been shown that the steric interaction between the methyl group of coordinated 2-methylimidazole and the *meso*-isopropyl substituent of iron(III) tetralkylporphyrin, or 2-methylbenzimidazole and the ortho methyl protons of tetramesitylporphyrin, stabilizes this unusual electronic structure.[17b,c] Both species, i.e., $[(TAP)Fe^{III}(2\text{-MeIm})_2]^+$ and $[(TMP)Fe^{III}(2\text{-MeBzIm})_2]^+$, exhibited the pyrrole resonances near or in the untypical diamagnetic region.[17]

Previously we have examined high- and low-spin iron(III) complexes of iron(III) chiroporphyrin, obtained from (1*R*)-*cis*-caronaldehyde acid methyl ester and pyrrole as the $\alpha\beta\alpha\beta$ atropisomer ($TMCPH_2$).[22] Tetramethylchiroporphyrin with its bulky cyclopropyl groups at the *meso* positions promoted the contribution of the less common $(d_{xz}d_{yz})^4(d_{xy})^1$ ground state of low-spin iron(III) porphyrins $[(TMCP)Fe^{III}(2\text{-MeIm})_2]^+$. However, even coordination of cylindrical cyanide anion in methanol or methylene dichloride was sufficient to generate bis(cyanide) low-spin TMCP complexes with the $(d_{xz},d_{xz})^4(d_{xy})^1$ electronic ground state. Thus we have concluded that the electronic effect of the replacement of the aryl substituents by alkyl groups combined with a steric *meso*-substituent−axial ligand interaction seem to be crucial in determination of the low-spin iron(III) electronic structure.[22] To explore further on this issue we have decided to investigate the coordination chemistry of iron(III) 5,10,15,20-tetracyclohexylporphyrin ((TCHP)Fe^{III}) (Chart 1).

The *meso*-tetracyclohexylporphyrin bears the characteristic features of a regular tetralkylporphyrin providing however the markedly smaller steric hindrance in comparison to the previously studied iron(III) chiroporphyrin. We have noticed a potential resemblance between tetracyclohexylporphyrin and tetraphenylporphyrin, in that both porphyrins contain six-membered rings at *meso* positions rendering two sides of porphyrin macrocycles equivalent, creating similar steric hindrance for axially coordinated ligands.

Chart 1

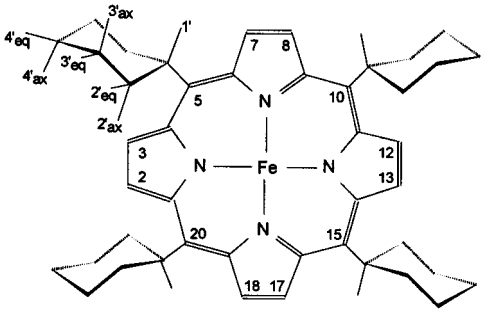

Here we report a detailed examination of the ^{1}H NMR spectra of a variety of high- and low-spin iron(III) 5,10,15,20-tetracyclohexylporphyrin complexes. The ^{1}H NMR spectroscopy has been shown to be a uniquely sensitive method for detecting and characterizing iron porphyrins. The hyperfine shift patterns that have been recorded for paramagnetic iron porphyrins are indicative for iron oxidation, spin, and ligation states.[18,19] The aim of this investigation was to elucidate the influence of the tetracyclohexylporphyrin on the electronic properties of its low-spin iron(III) complexes. Additionally the coordination of the external nitrogen bases, R-imidazoles, have been examined providing an insight into the correlation between the ground electronic state of iron(III) and the ^{1}H NMR pattern of axial ligands. Thus imidazole serves as a model for histidine which frequently is found as a ligand in low-spin iron(III) heme proteins although the corresponding ^{1}H NMR features have not been analyzed in the context of the less common low-spin iron(III) ground electronic state.[18,19,23,24]

Results and Discussion

Symmetry Analysis. The ^{1}H NMR data have been analyzed in the context of symmetry imposed by coordination of axial ligand(s) and rotation of the cyclohexyl substituent around the $C_{meso}-C_{1'}$ bond. The stereochemistry of equatorially coordinated 5,10,15,20-tetracyclohexylporphyrin (TCHP)Fe$^{III}X_n$ (X = axial ligand, n = 1 or 2) can be anticipated considering the X-ray structures of (TCHP)Zn^{II}.[25]

The bulky metalloporphyrin fragment is located in the equatorial position of the cyclohexyl substituent freezing a single chair conformation of the otherwise flexible cyclohexyl ring. With respect to a single $C_{1'}-C_{meso}$ bond two essentially different rotamers are expected, differentiated by the right (g) or left (−g) orientation of the 1-H′ proton (Chart 2) with a θ angle in the range 80° determined as by X-ray crystallography for Ni(II) or Zn(II) complexes.[25]

The slow rotation with respect of the $C_{1'}$-C_{meso} bond of the cyclohexyl group will create four atropisomers (g,g,g,g), (g,g,g,−g), (g,−g,g,−g), (g,g,−g,−g) of a (TCPH)Fe^{III} fragment formed in the first approximation in statistic proportions.

The pyrrole and 1′-H resonances offer a spectroscopic probe to get an insight into their formation as the corresponding resonances are located in suitable, well-separated spectral

(15) Simonneaux, G.; Hindre, F.; Le Plouzennec, M. *Inorg. Chem.* **1989**, *28*, 825.
(16) Guillemot, M.; Simonneaux, G. *J. Chem. Soc., Chem. Commun.* **1995**, 2093.
(17) (a) Nakamura, M.; Ikeue, T.; Fujii, H.; Yoshimura, T. *J. Am. Chem. Soc.* **1997**, *119*, 6284. (b) Nakamura, M.; Ikeue, T.; Neya, S.; Funasaki, N.; Nakamura, N. *Inorg. Chem.* **1996**, *35*, 3731. (c) Nakamura, M.; Nakamura, M. *Chem. Lett.* **1991,** 1885.
(18) Walker, F. A.; Simonis U. In *Biological Magnetic Resonance, Volume 12 NMR of Paramagnetic Molecules*; Berliner, L. J., Reuben, J., Eds.; Plenum Press: New York, 1993; p 133.
(19) La Mar, G. N.; Walker, F. A. In *The Porphyrins*; Dolphin, D., Ed.; Academic Press: New York, 1979; pp 61−312.
(20) (a) Stolzenberg, A. M.; Strauss, S. H.; Holm, R. H. *J. Am. Chem. Soc.* **1981**, *103*, 4763. (b) Coulter, E. D.; Sono, M.; Chang, C. K.; Lopez, O.; Dawson, J. H. *Inorg. Chim. Acta* **1995**, *240*, 603.
(21) Wojaczyński, J.; Latos-Grażyński, L.; Głowiak, T. *Inorg. Chem.* **1997**, *36*, 6299.
(22) Wołowiec, S.; Latos-Grażyński, L.; Mazzanti, M.; Marchon, J.-C. *Inorg. Chem.* **1997**, *36*, 5761.
(23) Liccocia, S.; Chatfield, M. J.; La Mar, G. N.; Smith, K.; Mansfield, K. E.; Anderson, R. R. *J. Am. Chem. Soc.* **1989**, *111*, 6087.
(24) Chacko, V. P.; La Mar, G. N. *J. Am. Chem. Soc.* **1982**, *104*, 7002.

Chart 2

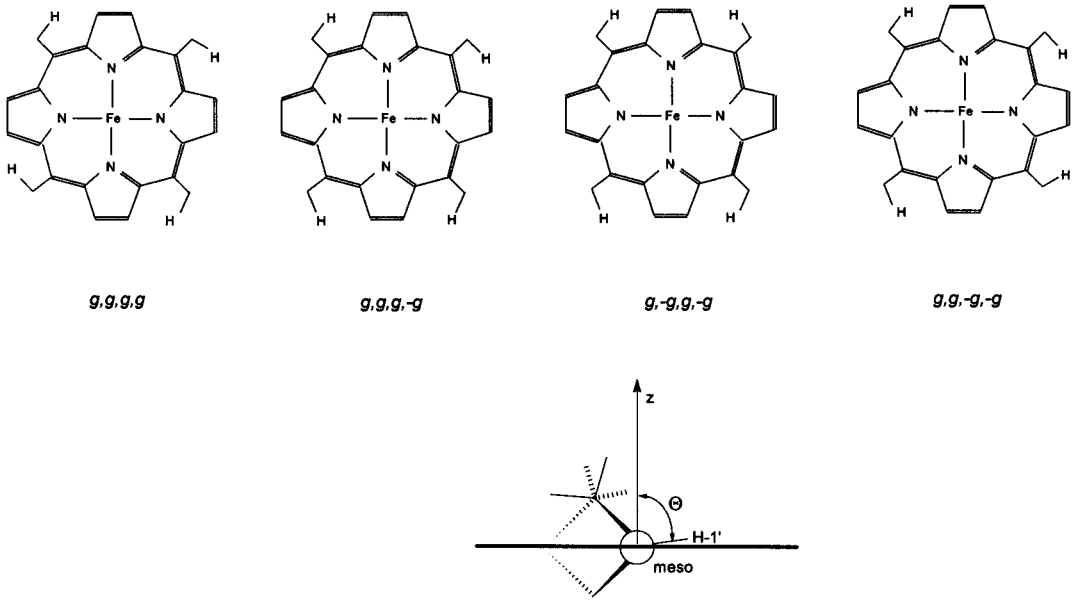

regions for both low-spin and high-spin iron(III) complexes. The number of the unequivalent components in the region of pyrrole and 1′-H (in parentheses) resonances, assuming the cylindrical symmetry of axial ligand(s), is as follows: (g,g,g,g), 2 (1); (g,g,g,−g), 8 (4), (g,−g,g−g), 2 (1), (g,g,−g,−g), 4 (2). As the paramagnetic shifts of atropisomers are typically dependent on their structure, the ^{1}H NMR spectra of (TCHP)-Fe^{III}X should show 16 pyrrole and 8 1′-H resonances.

Considering five-coordinated high-spin iron(III) complex it may be anticipated that the proton in the following pairs $2'_{eq}$-H, $2'_{ax}$-H, $3'_{eq}$-H, and $3'_{ax}$-H on each cyclohexyl ring will be distinguishable, due to the essentially perpendicular position of the cyclohexyl ring with respect to the porphyrin plane and the restricted rotation about the $C_{meso}-C_{1'}$ bond. On the other hand bis(cyanide) species will reveal the multiplicity of cyclohexyl resonances accordingly to that established for the 1′-H position.

The above presented consideration assumes the effectively symmetrical geometry of axial ligands. However coordination of 1,2-dimethylimidazole restricts rotation with respect to the Fe−N(Im) axis (vide infra) providing one more source of asymmetry. The additional factor increases the number of ^{1}H NMR distinguishable isomers to 10 (three for (g,g,g,−g), two for (g,−g,g,−g), four for (g,g,−g,−g) and one for (g,g,g,g)) producing for instance 34 unequivalent resonances assigned to 1′-H.

Molecular mechanics calculations have been used only to visualize a representative structure. In a minimization procedure we have used the standard MM+ parametrization of the Hyperchem program with an exception for the iron coordination environment where we have imposed constraints on bond distances consistent with the low-spin iron(III) state.[26,27] As a the starting point of molecular mechanics calculations, the X-ray structure of a high-spin iron(III) chiroporphyrin has been used but the cyclohexyl fragments replaced chiral *meso*-substituents to produce the (g,g,g,g) isomer.[22] Schematic views of the representative model are presented in Figure 1.

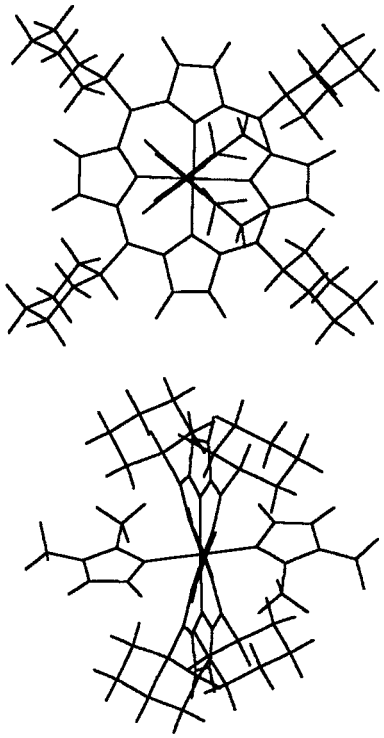

Figure 1. Schematic views of the representative [(TCHP)Fe^{III}(1,2-diMeIm)$_2$]$^+$ structure as obtained by molecular mechanics. The complex is shown in two essential projections presenting the top and side views of tetracyclohexylporphyrin.

In the course of our calculations, the planar 1,2-diMeIm ligands have been finally located within the grooves, which lie perpendicular each to other along the $C_{meso}-C_{meso}$ diagonals due to the distortion of the ligand from planarity. If fast on the NMR time scale, rotation of the cyclohexyl moiety with respect to the $C_{1'}-C_{meso}$ bond would simplify considerably the spectroscopic analysis, yielding effectively the spectral features typical of a planar symmetrical *meso* substituent. In such a case, a single pyrrole resonance and a single 1′-H resonance are expected for (TCHP)Fe^{III}Cl, [(TCHP)Fe^{III}(CN)$_2$]$^-$, [(TCHP)-Fe^{III}(ImH)$_2$]$^+$, and [(TCHP)Fe^{III}(1-MeIm)$_2$]$^+$ complexes. Accordingly four pyrrole resonances and two sets of 11 cyclohexyl

(25) Veyrat, M.; Ramasseul, R.; Marchon, J.-C. *New. J. Chem.* **1995**, *19*, 1199.
(26) Scheidt, W. R.; Lee, Y. J. *Struct. Bonding* **1987**, *64*, 1.
(27) Munro, O. Q.; Marques, H. M.; Debrunner, P. G.; Mohanrao, K.; Scheidt, W. R. *J. Am. Chem. Soc.* **1995**, *117*, 935.

Table 1. ^{1}H NMR Data for Iron(III) Tetracyclohexylporphyrin (Chemical Shifts in ppm)[a]

	assignment						
compd	β−H	1′-H	2′-H$_{eq}$	2′-H$_{ax}$	3′-H$_{eq}$	3′-H$_{ax}$	4′-H
(TCHP)Fe^{III}Cl	88.3	27.6	1.83	−0.26	9.61	3.05	3.12; 3.61
[(TCHP)Fe^{III}(CN)$_2$]$^-$ [b]	12.01	24.78	0.45	−1.12	7.47	1.96	2.21; 2.36
[(TCHP)Fe^{III}(CN)$_2$]$^-$ [c]	10.82	21.70	*d*	−0.54	6.54	*d*	*d*
[(TCHP)Fe^{III}(1-MeIm)$_2$]$^+$	4.24	15.49	1.03	−0.72	5.53	1.64	*d*
[(TCHP)Fe^{III}(HIm)$_2$]$^+$	2.81	13.79	0.97	−0.73	4.97	1.45	1.95; 1.84
[(TCHP)Fe^{III}(1,2-diMeIm)$_2$]$^+$	9.27; 6.39	19.8; 18.1	2.30	0.07	6.80	3.52	2.2
[(TCHP)Fe^{III}(1,2-diMeIm)$_2$]$^+$ [e]	7.6,[f1] 11.09 [f2]	23.71[g]	2.90; 1.84[g]	−0.25[g]	7.34; 7.06[g]	2.43; 2.3[g]	*d*
	6.2,[h1] 10.61[h2]	21.00[i]	2.61; 1.71[i]	0.95; −1.60[i]	7.79; 7.63[i]	1.20; 0.98[i]	

[a] In chloroform-*d* at 293 K unless stated differently. [b] KCN in CD_3OD. [c] (TBA)CN in CD_2Cl_2. [d] Overlapped with solvent or ligand resonances. [e] Data at 253 K, assignments arbitary assuming orientation of 1,2-diMeIm as in Figure 1: (*f*1) 2-H; (*f*2), 3-H; (*g*) set of 5,10-cyclohexyl resonances; (*h*1) 7-H; (*h*2) 17-H; (*i*) the set of 15,20-cyclohexyl resonances.

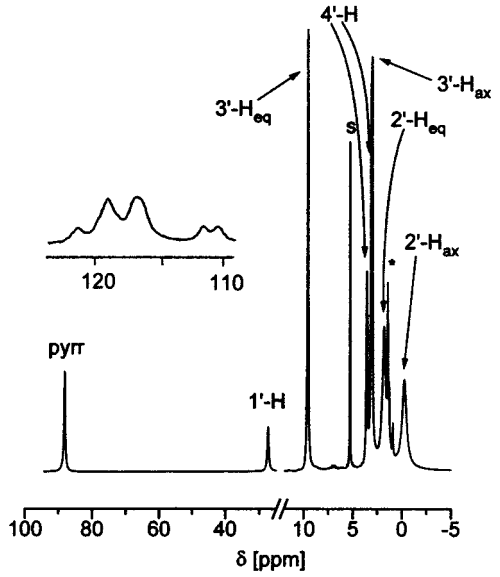

Figure 2. 300 MHz ^{1}H NMR spectrum of ((TCHP)Fe^{III}Cl in chloroform-*d* at 293 K. The inset presents the 1′-H region measured at 183 K demonstrating the spectrum complexity induced by slower rotation of the cyclohexyl moiety. The labeling of the cyclohexyl moiety follows that in Chart 1: pyrr, pyrrole β-H; s, $CHCl_3$, *, impurities.

resonances are expected for [(TCHP)Fe^{III}(1,2-diMeIm)$_2$]$^+$. We point out that the diastereotopic effect will preserve the intrinsic inequivalence of otherwise equivalent 2′$_{eq}$-H, 2′$_{ax}$-H, 3′$_{eq}$-H, and 3′$_{ax}$-H pairs of cyclohexyl protons even in the case of their fast rotation.

One-Dimensional ^{1}H NMR Studies of Iron(III) Tetracyclohexylporphyrin. Representative spectra of high-spin (TCHP)Fe^{III}Cl are shown in Figure 2. Resonance assignments which are given in Figure 2 and in Table 1 have been made on the basis of relative intensities and line width analysis. The spectral pattern is consistent with an effective C_{4v} symmetry. The ^{1}H NMR spectrum, collected at 293 K, resembles that one of a tetraphenyl analogue (TPP)Fe^{III}Cl. The pyrrole resonance is located in the similar spectral region although is noticeably more downfield shifted (88.3 ppm vs 80 ppm for (TPP)Fe^{III}Cl at 293 K).[18,19] The 1′-H resonance at 27.6 ppm is shifted downfield as expected for any *meso*-alkyl substituent of the high-spin iron(III) porphyrin.[22,28] As the temperature lowered, all resonances split due to the slower rotation of the cyclohexyl groups. The pyrrole proton resonance splitting observed at 183 K is presented in the inset of Figure 2 and reflects the participation of the predicted atropisomers.

Addition of an excess potassium cyanide to a solution of (TCHP)Fe^{III}Cl in methanol-d_4 results in its conversion to a six-coordinate low-spin complex: [(TCHP)Fe^{III}(CN)$_2$]$^-$. A titration of (TCHP)Fe^{III}Cl with (TBA)CN in dichloromethane-d_2 produced [(TCHP)Fe^{III}(CN)$_2$]$^-$ as well. Usually low-spin iron(III) porphyrins formed by coordination of two cyanide ligands result in very narrow, paramagnetically shifted resonances due to the optimal relaxation properties.[29] The representative ^{1}H NMR spectrum for [(TCHP)Fe^{III}(CN)$_2$]$^-$ is shown in Figure 3 as the top projection for a 2-D map. The peculiar position of the pyrrole resonances at 12.01 ppm (293 K) is of importance to describe the electronic structure. This resonance is accompanied by a downfield shifted 1′-H resonance at 24.78 ppm and a group of remaining *meso*-alkyl resonances located in the diamagnetic region. A comparison of the spectra collected in dichloromethane-d_2 and methanol-d_4 reveals some differences in isotropic shifts accounted for by hydrogen bonding which is present in methanol but is absent in dichloromethane. It has been demonstrated earlier that hydrogen bonding to the cyanide ligand generally results in a decrease of the [(TPP)Fe^{III}(CN)$_2$]$^-$ isotropic shifts.[29a]

Titration of (TCHP)Fe^{III}Cl by imidazole or its methyl-substituted derivatives converts high-spin iron(III) tetracyclohexylporphyrin into the respective low-spin counterparts. Complete conversion has been achieved for a 1:4 (TCHP)Fe^{III}Cl: R-imidazole molar ratio even for the most sterically hindered 1,2-diMeIm. In each investigated case we have confirmed the coordination of two R-Im ligands by integration of the pyrrole and R-imidazole ligand resonances. The ^{1}H NMR spectra for a series of [(TCHP)Fe^{III}(R-Im)$_2$]$^+$ complexes are shown in Figure 4. The resonance assignments which are given above selected peaks have been made on the basis of relative intensities and line width analysis and have been unambiguously confirmed by 2D NMR experiments. The imidazole resonances have been identified through suitable deuteration(s). The spectra obtained for imidazole-2-*d* and imidazole-d_3 are shown in traces c and d of Figure 4. The resonance of 2-H is readily assigned since its intensity diminished in the spectrum of [(TCHP)Fe^{III}(Im-2-*d*)$_2$]$^+$. All but the 1-NH imidazole resonance are missing in the spectrum of the imidazole-d_3 adduct. The 4-H resonance is assigned on the basis of its line width (181 Hz at 230 K), which is similar to that of the 2-H resonance (140 Hz). Both are expected to be at similar distances from the iron(III) ion, and both should have comparable line widths that are greater than those of the other imidazole resonances (5-H, 38.4 Hz, and NH, 47.2 Hz).

(28) Wołowiec, S.; Latos-Grażyński, L.; Serebrennikova, O. V.; Czechowski, F. *Magn. Reson. Chem.* **1995**, *33*, 34

(29) (a) La Mar, G. N.; Del Gaudio, J.; Frye, J. S. *Biochim. Biophys. Acta* **1977**, *498*, 422. (b) La Mar, G. N.; Viscio, D. B.; Smith, K. M.; Caughey, W. S.; Smith, M. L. *J. Am. Chem. Soc.* **1978**, *100*, 8065.

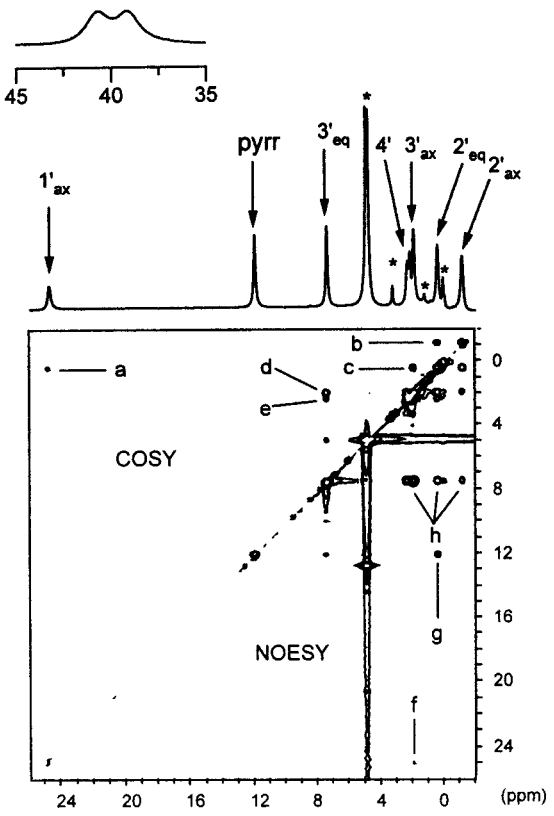

Figure 3. 2D ^{1}H NMR spectra of $[(TCHP)Fe^{III}(CN)_2]^+$ in methanol-d_4 at 293 K. The top-left triangle presents the COSY map, and the bottom-right part demonstrates the NOESY experiment. The most characteristic cross-peaks are labeled as follows. COSY: a, 1′-H-2′eq-H; b, 2′eq-H−2′ax-H; c, 2′eq-H−3′ax-H; d, 3′ax-H−3′eq-H; e, 4′eq-H (4_{ax}-H)−3′eq-H. NOESY: g, β-H−2′eq-H; f, 1′ax-H−3′ax-H; h, a series of NOE cross-peaks between 3′eq-H and 2′−H, 3′ax-H, and 4′−H. The 1-D ^{1}H NMR spectrum is presented at top of the 2-D map together with the inset demonstrating the split of 1′-H resonances at 193 K. The labeling follows that of Figure 2.

Fast rotation around Fe−N(R-imidazole) bond generates, as a resultant, the ^{1}H NMR pattern accounted for by an effectively symmetrical ligand. The steric hindrance of 1,2-diMeIm slowed such a dynamic process to an extent that the pattern corresponding to the structure shown at Figure 1 has been observed in the 240−293 K range presuming the fast rotation of the cyclohexyl moiety. Below 230 K the relevant atropisomers exhibit distinct spectra as revealed by a complex multiplets at the pyrrole and 1′-H regions in the inset of Figure 5. The splitting of 1′-H resonances shown for the $[(TCHP)Fe^{III}(CN)_2]^-$ in the inset of Figure 3 is due to the same phenomenon.

The effects of temperature on the ^{1}H NMR spectra of $[(TCHP)Fe^{III}(CN)_2]^-$ and $[(TCHP)Fe^{III}(1,2\text{-diMeIm})_2]^+$ are shown in Figure 6, where the pyrrole and 1′-H chemical shifts are plotted versus 1/*T*. In general these plots are not linear as would be expected according to the Curie law for simple paramagnetic complexes. Rather they show noticeable curvatures.

2D NMR Studies of Low-Spin Iron(III) Tetracyclohexylporphyrin. The complete assignments of resonances required an application of two-dimensional ^{1}H NMR techniques. Routinely the 2D NMR spectra have been collected at several temperatures to achieve the optimal spread of a one-dimensional spectrum prior to two-dimensional analysis. Here we present only the most fundamental steps of the resonance assignments carried out in the representative case of $[(TCHP)Fe^{III}(CN)_2]^-$ as shown in the combined COSY/NOESY map in Figure 3.

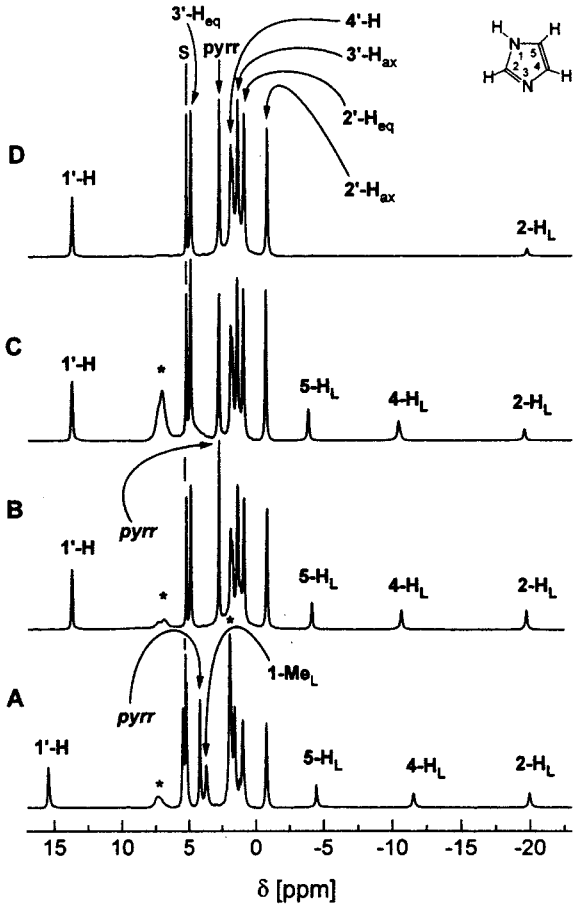

Figure 4. 300 MHz ^{1}H NMR spectra: (A) $[(TCHP)Fe^{III}(1\text{-MeIm})_2]^+$; (B) $[(TCHP)Fe^{III}(Im)_2]^+$; (C) $[(TCHP)Fe^{III}(Im\text{-}2\text{-}d)_2]^+$; (D) $[(TCHP)Fe^{III}(Im\text{-}d_3)_2]^+$ in chloroform-*d* at 293 K.

The COSY experiment has been effective in connecting the protons of the cyclohexyl fragment once the 1′-H resonance has been located at 24.78 ppm (293 K). This proton is scalar coupled to $2'_{eq}$-H (a), which is geminally coupled with $2'_{ax}$-H (b) and vicinally coupled with the $3'_{ax}$-H (c), the latter being again geminally coupled with the $3'_{eq}$-H (d). Finally, two closely located resonances of intensity corresponding both to four protons are assigned to $4'_{eq}$-H and $4'_{ax}$-H (not well-resolved) which show the scalar coupling with $3'_{eq}$-H (e). Thus the unique resonance (eight proton intensity) at 12 ppm has been assigned to β-H protons. In the NOESY part of the map the expected internal *meso*-cyclohexyl spatial contact (g) between pyrrole β-H and $2'_{eq}$-H protons has been established as suggested by molecular modeling and the crystal structure of $(TCHP)Ni^{II}$.[25] In addition the following contacts have been determined: $1'_{ax}$-H and $3'_{ax}$-H (f) and a series of NOE cross-peaks h between $3'_{eq}$-H and 2′-H, $3'_{ax}$-H, and 4′-H. The connectivity pattern is summarized in Scheme 1.

2D NMR Studies of $(TCHP)Fe^{III}(1,2\text{-diMeIm})_2$. To provide the best conditions for two-dimensional studies we have selected the temperature (253 K) where the rotation of the cyclohexyl ring is fast enough to allow the relatively high-symmetry spectrum.

The COSY map (Figure 5) demonstrates a single scalar cross-peak h correlating 2-H and 3-H resonances allowing unambiguous assignment of a 2,3-H pyrrole pair. The scalar cross-peaks c−g within the cyclohexyl substituent identified the resonances within the 4, −2 ppm crowded region. Cross-peaks a and b correspond to scalar coupling between 1-Me (L) and vicinal

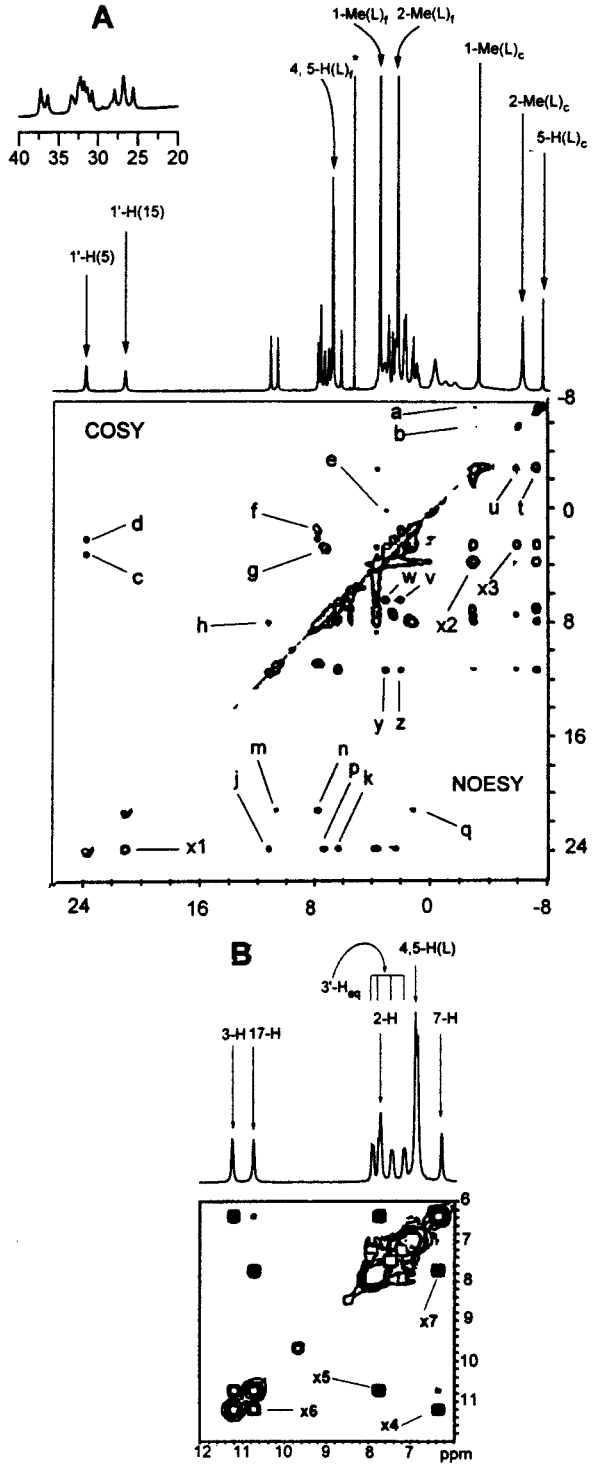

Figure 5. 2D ^{1}H NMR spectra of [(TCHP)Fe^{III}(1,2-diMeIm)$_2$]$^+$ in dichloromethane-d_2 at 253 K. (A) The top-left triangle presents the COSY map, and (B) bottom part demonstrates the NOESY experiment. The inset at the top of the 1D ^{1}H NMR spectrum at (A) demonstrates the complexity of the 1′-H region of the spectrum at 193 K due to slower rotation of the cyclohexyl moiety. The most characteristic cross-peaks are labeled as follows. COSY: h, 2-H−3-H, c−g, cross-peaks within the cyclohexyl substituent; a, 1-Me (L)−5-H (L), b, 1-Me−2-Me (L). NOESY map: EXSY cross-peaks x_2, 1-Me(L)$_f$−1-Me(L)$_c$; x_3, 2-Me(L)$_f$−2-Me(L)$_c$; x_1, 5 (10) and 15 (20) 1′-H protons; x_4−x_7 the series between pyrrole β-H (x_4; 3 (12) vs 7 (8); x_5, 17 (18) vs 2 (13), x_6, 3 (12) vs 17 (18); x_7, 2 (13) vs 7 (8)). NOE cross-peaks: intra-axial-ligand NOE cross-peaks (t, u) and intra-*meso*-cyclohexyl cross-peaks p, q; j and k, 3 (12)-H and 7 (8)-H and 1′-H (*meso*-5 or 10); n and m, 2 (13) and 18 (17)-H and 1′-H (*meso*-15 or 20); two pairs w, v and z, y, 2′$_{eq}$-5 (10) cyclohexyl moiety and flanking pyrrole β-H.

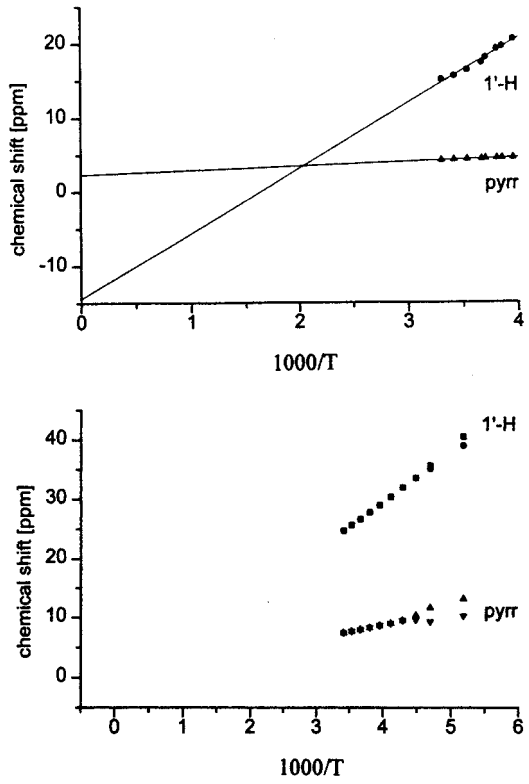

Figure 6. Temperature dependence of the chemical shifts of (A, bottom) pyrrole and 1′-H resonances of [(TCHP)Fe^{III}(CN)$_2$]$^-$ in methanol-d_4 and (B, top) pyrrole and 1′-H resonances of [(TCHP)Fe^{III}-(1-MeIm)$_2$]$^+$ in dichloromethane-d_2. The individual assignments are shown. The solid lines are shown for illustrative purpose only.

Scheme 1

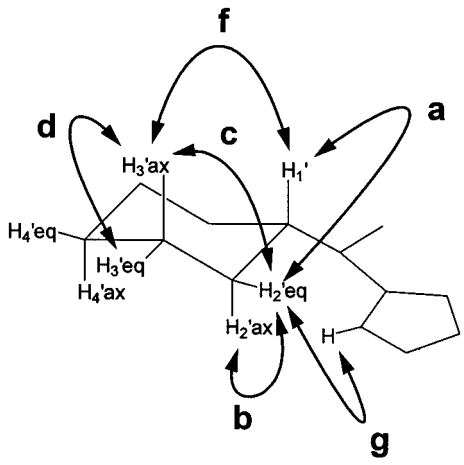

5-H (L) and 2-Me (L) of axial 1,2-diMeIm ligand, respectively (Figure 5A, left upper triangle). The connectivity is shown at Scheme 2.

The steric hindrance of 2-methyl renders the rotation of axial ligands slow on the ^{1}H NMR time scale to show separate resonances for unequivalent positions at 253 K. Moreover, the rotation is fast enough to observe the EXSY cross-peaks (labeled consequently x_n) between corresponding resonances in the NOESY map. The EXSY cross-peaks x_2 and x_3 between coordinated and free methyl groups of axial ligand allow to identify 1-Me(L) and 2-Me(L) resonances of the [(TCHP)Fe^{III}-(1,2-diMeIm)$_2$]$^+$ complex. Such an exchange is typical for low-spin iron(III) porphyrins.[17,30d,31−33] The EXSY cross-peak x_1 between 5 (10) and 15 (20) 1′-H protons (Figure 5A) and the series of x_4−x_7 ones (Figure 5B, expanded 12−6 region of

Scheme 2

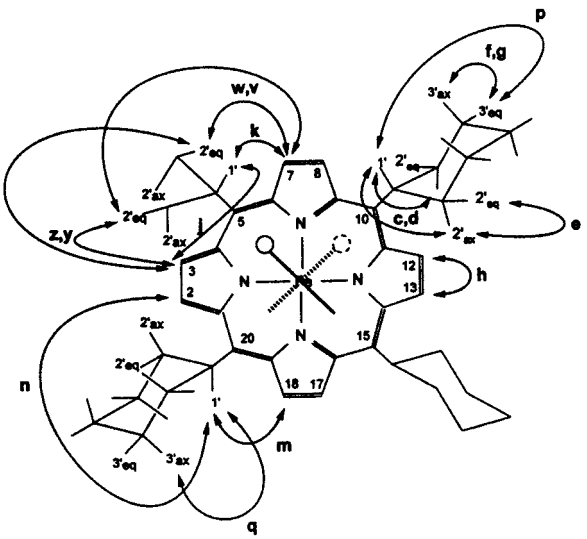

NOESY map) between pyrrole β-H (x_4; 3 (12) vs 7 (8), x_5; 17 (18) vs 2 (13), x_6; 3 (12) vs 17 (18), and x_7; 2 (13) vs 7 (8)) are consistent with the chemical exchange between two isomers mutually convertible by a 180° rotation of one of axial ligands. The chemical exchange between two isomers which require 180° rotation of two axial ligands produced EXSY cross-peaks of lower intensity, one of which (not labeled, 17 (18) vs 7 (8) β-H) is observed at the threshold applied. Only some of NOE cross-peaks observed are labeled to demonstrate the spatial contacts within the molecule. Apart from strong intra-axial-ligand NOE cross-peaks (t and u) and intra-*meso*-cyclohexyl cross-peaks p and q, the series of NOE cross-peaks between corresponding pyrrole β-H and 1′-H, as well as those between pyrrole β-H and $2'_{eq}$-H, are observed, namely as follows: j and k corresponding to contacts between 3 (12)-H and 7 (8)-H and 1′-H (*meso*-5 or 10); n and m corresponding to contacts between 2 (13) and 18 (17)-H and 1′-H (*meso*-15 or 20); two pairs w, v and z, y of cross-peaks between both $2'_{eq}$ of 5 (10) cyclohexyl moieties and flanking the pyrrole β-H. Those two pairs of cross-peaks are consistent with the freely rotating cyclohexyl model. We have not identified the reliable NOE cross-correlation between the 2-Me resonance of the axial ligand and the porphyrin protons which would point to the spatial proximity between the selected fragments of the complex. Consequently, it precludes the unambiguous determination of the 1,2-diMeIm ligand orientation with respect to the porphyrin skeleton.

The rotation of 1,2-diMeIm, although relatively slow as we can see a set of resonances representative for four equivalent rotamers in the very large (183−303 K) temperature range, has been confirmed by EXSY correlation peaks at the NOESY spectra. This is the second example of such a behavior in the low-spin iron(III) porphyrin series. Previously we have determined the similar stability for $[(TMCP)Fe^{III}(1,2\text{-diMeIm})_2]^+$. It was also found that coordination of sterically hindered imidazoles to form $[(TMP)Fe^{III}(2\text{-MeIm})_2]^+$,[30a,f,g,34a] $[(TMP)Fe^{III}(2\text{-MeBzIm})_2]^+$,[34b] and $[(TAP)Fe^{III}(2\text{-MeIm})_2]^+$ [17] induced the S_4 deformation and restricted rotation around the Fe−N bond but only at low-temperature limits. Analogously to $[(TMCP)Fe^{III}(1,2\text{-diMeIm})_2]^+$, we assume that the dynamic rearrangement $[(TCHP)Fe^{III}(1,2\text{-diMeIm})_2]^+$ requires the intermediate form which would facilitate the exchange between $[(TCHP)Fe^{III}(1,2\text{-diMeIm})_2]^+$ isomers. The rotation will create successive switching of the up/down ruffling distortion at the particular *meso* positions. The recent analysis of factors which are instrumental in determination of the core geometry demonstrated that ligand−porphyrin non bonding interactions including *meso*-substituents are the primary determinant of core conformation.[27]

Electronic Structure of Low-Spin Iron(III) Tetracyclohexylporphyrin. It has been demonstrated that the major contribution to the isotropic shift of the pyrrole protons of low-spin iron(III) tetrarylporphyrins is of contact origin.[18,19] Generally negligible dipolar shifts were observed for iron porphyrin systems with a pure $(d_{xz}d_{yz})^4(d_{xy})^1$ ground state.[14−16] Thus the contribution of the dipolar shift in the isotropic shift of $[(TCHP)Fe^{III}X_2]$ may be expected to increase in the axial ligand series $CN^-(CD_3OD) \simeq CN^-(CD_2Cl_2) <$ 1-MeIm, ImH < 1,2-diMeIm, following the order of the pyrrole isotropic shifts. The isotropic shift pattern reflects mainly the spin density distribution due to the contact mechanism. The sign alternation of isotropic shifts, measured for *meso*-cyclohexyl resonances with respect to $(TCHP)Zn^{II}$, supports this conclusion as the dipolar contribution would generate the identical signs of their isotropic shifts.[25]

Generally the ground state of the low-spin iron(III) porphyrin can be described by two limiting electronic configurations[12−17] $(d_{xy})^2(d_{xz}d_{yz})^3$ and $(d_{xz}d_{yz})^4(d_{xy})^1$ distinguishable by ^{1}H NMR spectroscopy.[12−16,18] In the first case one can expect the upfield position of the pyrrole resonances due to P → Fe π delocalization through the $3e_g(\pi)$ filled orbitals of porphyrins. In the second case, the specific downfield position of the pyrrole resonances and strong contact shift of the *meso* substituents are expected. Such a spin density distribution including the large spin density at the *meso* positions is indicative of the $(d_{xz}d_{yz})^4(d_{xy})^1$ electronic state with the partial a_{2u} π-cation radical character.[14b,18] The large spin density at the *meso* positions will translate into the unusually large downfield shift of the corresponding 1′-H resonances.[22,35] The shift value depends on the orientation of 1′-H with respect to the porphyrin macrocycle as described by a dihedral angle θ between the plane determined by the p_z axis of the *meso* carbon (C_{meso}) and the $C_{meso}-C_{1'}$ bond and the $C_{meso}-C_{1'}-H$ bonds.[22] The value of θ measured from the models approaches 80° for all investigated species as required by the tendency of the bulky *meso*-alkyl fragment to be located furthest away from the porphyrin plane. Consequently the position of the 1′-H resonances reflects primary the effects which are related to changes of the spin density accompanying the modification of the ground electronic state. In general the large downfield isotropic shift of the 1′-H protons is accompanied by the smaller upfield shift (as far as

(30) (a) Walker, F. A.; Simonis, U. *J. Am. Chem. Soc.* **1991**, *113*, 8652. (b) Lin, Q.; Simonis, U.; Tipton, A. R.; Norvell, C. J.; Walker, F. A. *Inorg. Chem*. **1992**, *31*, 4216. (c) Simonis, U.; Dallas, J. Walker, F. A. *Inorg. Chem*. **1992**, *31*, 5349. (d) Simonis, U.; Lin, Q.; Tan, H.; Barber, R. A.; Walker, F. A. *Magn. Reson. Chem.* **1993**, *31*, S133. (e) Tan, H.; Simonis, U.; Shokiriev, N. V.; Walker, F. A. *J. Am. Chem. Soc.* **1994**, *116*, 5784. (f) Shokhirev, N. V., Shokhireva, T. Kh., Polam, J. R., Watson, C. T., Raffii, K., Simonis, U., Walker, F. A. *J. Phys. Chem. A* **1997**, *101*, 2778. (g) Momot, K. I., Walker, F. A. *J. Phys. Chem. A* **1997**, *101*, 2787.

(31) Walker, F. A.; Simonis, U.; Zhang, H.; Walker, J. M.; McDonald Ruscitti, T.; Kipp, C.; Amptuch, M. A.; Castillo, B. V., III; Cody, S. H.; Wilson, D. L.; Graul, R. E.; Yong, G. J.; Tobin, K.; West, T. J.; Barichiewich, B. A. *New. J. Chem.* **1992**, *16*, 609.

(32) Nakamura, M.; Tajima, K.; Tada, K.; Ishizu, K.; Nakamura, N. *Inorg. Chim. Acta* **1994**, *224*, 113.

(33) Saterlee, J. D.; La Mar, G. N.; Bold, T. J. *J. Am. Chem. Soc.* **1977**, *99*, 1088.

(34) (a) Nakamura, M.; Groves, J. T. *Tetrahedron* **1988**, *44*, 3225. (b) Nakamura, M. *Bull. Chem. Soc. Jpn.* **1995**, *68*, 197.

(35) . Pignolet, L. H.; La Mar, G. N. In *NMR of Paramagnetic Molecules*, La Mar, G., Horrocks, W. D., Jr., Holm, R. H., Eds.; Academic Press: New York, 1973; p 357.

Table 2. ^{1}H NMR Data for R-Imidazol Coordinated to Iron(III) Tetracyclohexylporphyrin (Chemical Shifts in ppm)[a,b]

	assignment						
compd	1-H	2-H	4-H	5-H	1-CH_3	2-CH_3	β-H
[(TCHP)Fe^{III}(1-MeIm)$_2$]$^+$		−19.91 (−20.86)	−11.50 (−11.98)	−4.42 (−8.85)	3.74 (2.14)		4.24 (−4.46)
[(TCHP)Fe^{III}(HIm)$_2$]$^+$	0.97 (−11.73)	−19.67 (−20.62)	−10.58 (−11.06)	−4.05 (−4.47)			2.81 (−5.89)
[(TCHP)Fe^{III}(1,2-diMeIm)$_2$]$^+$			*c*	−4.86 (−3.86)	−1.55 (−3.15)	−3.80 (−1.24)	9.27; 6.39 (0.57, −2.31)
[(TMCP)Fe^{III}(1-MeIm)$_2$]$^+$		−15.68 (−16.63)	0.0 (−0.48)	−1.64 (−6.07)	11.04 (9.44)		−8.31; −8.18 (−17.01, −16.88)
[(TMCP)Fe^{III}(HIm)$_2$]$^+$	*c*	−14.41 (−15.36)	2.02 (−1.54)	1.24 (−3.19)			−10.16, −9.97 (−18.87, −18.67)
[(TMCP)Fe^{III}(2-MeImH)$_2$]$^+$	*c*		11.77 (10.01)[d]	*c*		*c*	−7.83, −7.22, −4.11, −4.11 (−16.53, −15.92, −12.81, −12.81)[d]
[(TMCP)Fe^{III}(1,2-diMeIm)$_2$]$^+$			9.49 (9.01)	−0.32 (−4.85)	4.15 (2.55)	0.26 (2.82)[d]	−4.93, −4.08, −0.99, −0.66 (−13.63, −12.78, −9.69, −9.36)[d]
[(TPP)Fe^{III}(RIm)$_2$]$^+$ [e]	(−9.6)	(−28.0)	(−8.2)	(−7.6)	(10.3)	(12.0)	(−19.5)

[a] In chloroform-*d* at 293 unless stated differently. [b] In parentheses the isotropic shift is given as referenced to diamagnetic ruthenium(II) complexes from: Faller, J. W.; Chen, C. C.; Malerich, J. C. *J. Inorg. Nucl. Biochem.* **1979**, *11*, 151. [c] Not assigned. [d] The data for one isomeric form are given. [e] Contact shift from ref 19.

the absolute value is concerned) of the pyrrole protons. Similar trends have been previously determined for (TMCP)Fe^{III} complexes[22] although the shift of their 1′-H resonances is markedly larger when compared to analogous complexes of (TCHP)Fe^{III}. This difference is easily explained by θ approaching 0° for (TMCP)Fe^{III} but 80° for (TCHP)Fe^{III}.[22,25]

In the (TMCP)Fe^{III}X$_2$ series we have encountered two examples relevant to the two extreme ground electronic states $(d_{xy})^2(d_{xz}d_{yz})^3$-[(TMCP)Fe^{III}(1-MeIm)$_2$]$^+$ and $(d_{xz}d_{yz})^4(d_{xy})^1$-[(TMCP)Fe^{III}(CN)$_2$]$^-$ in methanol-d_4. The ^{1}H NMR patterns of the low-spin 2-MeIm or 1,2-diMeIm complexes corresponded to an intermediate situation where both electronic structures are of comparable importance. Thus, low-spin iron(III) tetracyclohexylporphyrin demonstrates a more pronounced tendency to generate the $(d_{xz}d_{yz})^4(d_{xy})^1$ contribution for the identical ligand series.

The curvature of the plots of isotropic shifts vs T^{-1} for the most sensitive 1′-H resonances and anti-Curie behavior of pyrrole resonances for [(TCHP)Fe^{III}(1-MeIm)$_2$]$^+$ can be accounted for by the complex electronic structure of the investigated species (Figure 6). Accordingly the populations of $(d_{xy})^2(d_{xz}d_{yz})^3$ and $(d_{xz}d_{yz})^4(d_{xy})^1$ electronic states vary according to the Boltzmann distribution.[22,36]

Finally the contribution of the $(d_{xz}d_{yz})^4(d_{xy})^1$ state may be qualitatively probed by the analysis of the isotropic shift of the imidazole ligands. It has been widely accepted that the contact shifts of imidazole ligands results from the Im → Fe porphyrin π bonding and is effective when the d_π orbitals contain unpaired electron density, i.e., for the $(d_{xy})^2(d_{xz}d_{yz})^3$ configuration.[18] The contact contributions are typically negative at all ring positions. In addition the contact shift demonstrated the clear evidence of reversal of sign for methyl substitution. Contrary, the unpaired spin density cannot be directly transferred into the imidazole fragment if the $(d_{xz}d_{yz})^4(d_{xy})^1$ distribution is solely operating as the d_{xy} orbital which does not overlap with π or π^* orbitals of imidazoles. The alternative Fe → π-back-bonding from $(d_{xz}d_{yz})^4$ should produce possibly the sign reversal when compared to typical iron(III) complexes. Therefore the upfield shift of the 1-H, 2-H, 4-H, and 5-H resonances, although resembling strongly that one established for a large variety of the low-spin iron(III) porphyrins, seems to be contradictory to the markedly diminished upfield contact shift of pyrrole protons. Furthermore, the replacement of the imidazole proton by a methyl group results in the isotropic shift of the methyl group which is 1 order of magnitude smaller than that for the replaced proton. On the other hand the similar absolute values for CH and C−CH_3 protons have been determined in the case for [(TPP)Fe^{III}(R-Im)$_2$]$^+$.[18,19,23,24,37,38]

These observations strongly suggest that the contribution of the new mechanism of axial ligand contact shifts should be considered for the novel ground electronic state of bis(imidazole)iron(III) porphyrins. Thus we have invoked the known pathway of spin density transfer, namely, a σ-delocalization which is usually neglected for low-spin bis(imidazole)iron(III) porphyrins.[18,19] Actually the continuous change of the π- versus σ-mechanism seems to be adequate to account for the observed changes of isotropic shifts (Table 2). Previously the contact shift of the pyridine ligands in [(TPP)Fe^{III}(R-py)$_2$]$^+$ has been accounted for by an increase of σ-delocalization once the $(d_{xz}d_{yz})^4(d_{xy})^1$ population increased.[18] Comparison of the measured contact shifts with those reported earlier for imidazole adducts of d^6 high-spin iron(II) porphyrins,[39] high-spin iron(II) *N*-methylporphyrins,[40] d^8 high-spin nickel(II) 21-thia- and 21-selenaporphyrins,[41] and other iron(II) and nickel(II) imidazole complexes[42] reveals some similarities in pattern but apparent differences in signs and magnitudes. The implication is that the mode of spin delocalization in the imidazole ligands is similar. However for the high-spin d^6 iron(II) coordination and high-spin d^8 nickel(II) coordination the shifts are all in the

(36) Shokiriev, N. V.; Walker, F. A. *J. Phys. Chem.* **1995**, *99*, 17795.
(37) Sattterlee, J. D.; La Mar, G. N. *J. Am. Chem. Soc.* **1976**, *98*, 2804.
(38) Balch, A. L.; Renner, M. W. *Inorg. Chem.* **1986**, *25*, 303.
(39) Goff, H. M.; La Mar, F. N. *J. Am. Chem. Soc.* **1978**, *100*, 1112.
(40) Balch, A. L.; Chan, Y.-W.; La Mar, G. N.; Latos-Grażyński, L.; Renner, M. W. *Inorg. Chem.* **1985**, *24*, 1437
(41) (a) Lisowski, J.; Latos-Grażyński, L.; Szterenberg, L. *Inorg. Chem.* **1992**, *31*, 1934. (b) Latos-Grażyński, L.; Pacholska, E.; Chmielewski, P.; Olmstead, M. M.; Balch, A. L. *Inorg. Chem.* **1996**, *35*, 566
(42) (a) Wicholas, M.; Mustatich, R.; Johnson, B.; Smedley, T.; May, J. *J. Am. Chem. Soc.* **1975**, *97*, 2113. (b) Wu, F.-J.; Kurtz, D. M., Jr. *J. Am. Chem. Soc.* **1989**, *111*, 6563. (c) Tovrog, B. S.; Drago, R. S. *J. Am. Chem. Soc.* **1974**, *96*, 2804. (d) Claramunt, R.-M.; Elquero, J.; Jacquier, R. *Org. Magn. Reson.* **1971**, *3*, 595. (e) Tovrog, B. S., Drago, R. S. *J. Am. Chem. Soc.* **1977**, *99*, 2203. (f) Wu, F.-J.; Kurtz, D. M., Jr. *J. Am. Chem. Soc.* **1989**, *111*, 6563.

opposite direction, which is downfield. This is also entirely reasonable, and indeed, opposite signs for spin density transfer to ligands have been predicted for high-spin d^6, d^8, and low-spin d^5 complexes.[43] The ligand to metal σ-bonding involves a half-occupied d_{z^2} orbital for Ni^{II} or Fe^{II} but an empty one for low-spin iron(III). Accordingly the first situation promotes β-spin density transfer where the α-spin transfer is preferred for ls iron(III) due to the $(d_{xy})^1$ electron in the second case. Similar sign reversals have been determined for adamantane bound to low-spin d^5 iron(III) as compared to azaadamantane coordinated to high-spin nickel(II).[44,45]

Conclusion. Low-spin iron(III) tetracyclohexylporphyrin and iron(III) chiroporphyrin complexes exhibit electronic properties considerably different from those of the analogous low-spin iron(III) tetrarylporphyrins. In the first place the electronic effect of the replacement of the aryl substituents by alkyl groups seems to be crucial. In the case of the R-imidazole ligands, the impact of porphyrin ruffling is of importance. The steric bulkiness of 1,2-diMeIm is required to freeze a favorable configuration, even at room temperature for both tetraalkylporphyrins, providing the perpendicular orientation of two imidazole planes which seems to be instrumental[14] in the stabilization of the rare $(d_{xz}d_{yz})^4(d_{xy})^1$ electronic state. However even relatively freely rotating R-imidazoles of $[(TCHP)Fe^{III}(1\text{-}MeIm)_2]^+$ are sufficient to stabilize this peculiar electronic state. The hyperfine shift pattern for imidazole ligands combined with a relatively small upfield contact shift of pyrrole resonances presents a useful probe for detecting such a ground state in hemoproteins by ^1H NMR spectroscopy, assuming that the small shift of pyrrole resonance is convertible into a small shift of porphyrin methyl resonances. Our investigations offer the alternative to account for an isotropic shift pattern of model species bearing the characteristic ^1H NMR features of $[(TCHP)Fe^{III}(Im)_2]^+$.

Experimental Section

Materials. 5,10,15,20-Tetracyclohexylporphyrin was obtained as previously described.[25] $(TCHP)Fe^{III}Cl$ was prepared by iron insertion into $TCHPH_2$ using known procedures.[22] Imidazole, 2-methylimidazole, 1-methylimidazole, 1,2-dimethylimidazole, and tetrabutylammonium cyanide ((TBA)CN) were used as received from Aldrich. Imidazole-2-*d* (Im-2-*d*) and imidazole-d_4 (Im-d_4) were prepared according to reported methods,[46] with a 50% deuteration at C_2. Imidazole-d_4 was used as a source of imidazole-d_3 since the ND is easily replaced by the residual water in solution to form NH. Methanol-d_4 (Glaser AG) has been used as received. Chloroform-*d* (Glaser AG) and dichloromethane-d_2 (Aldrich) were dried before use by passing through basic alumina.

The dicyano-ligated complexes of the investigated iron(III) porphyrin were prepared by dissolution of 2−3 mg of the respective high-spin complex in 0.4 mL of methanol-d_4 saturated with KCN. The titration of 2−3 mg of $(TCHP)Fe^{III}Cl$ in the respective solvent with nitrogen bases or (TBA)CN was applied to generate low-spin complexes.

NMR Experiments. ^1H NMR spectra were recorded on a Bruker AMX spectrometer operating in the quadrature mode at 300 MHz. The residual ^1H NMR resonances of the deuterated solvents ($CHCl_3$ or CHD_2OD) were used as a secondary reference. Magnitude COSY spectra were obtained after collecting the standard 1D reference spectra. The 2D COSY spectra were usually collected by use of 1024 points in t_2 over the desired bandwidth (to include all desired peaks) with 512 t_1 blocks and 40−200 scans per block in which 4 dummy scans were included. Repetition time was 200 ms in all cases. Prior to Fourier transformation, the 2D matrix was multiplied in each dimension with a 30° shifted sine-bell squared window function and zero-filled to obtain a 1024 × 1024 word square matrix. The NOESY (NOESYTP) were accumulated by use 512 points in t_2 and 1024 in t_1 and 32 scans per t_1 block. Prior to Fourier transformation the 2D matrix was multiplied in each dimension with a 30° shifted sine-bell squared window function and zero-filled to obtain a 1024 × 1024 word square matrix. Experimental parameters were varied to obtain best resolution and the signal-to-noise mode. Usually the repetition time was equal 200 ms. The mixing time was varied in the 15−150 ms range. The NOESY spectra were processed in the phase-sensitive or magnitude modes.

Molecular Mechanics Calculations. Molecular mechanics calculations using the HyperChem software (Autodesk) were carried out and displayed on a PC 486 computer. The standard MM+ force field, with the constrains set on the coordination bonds to achieve a low-spin iron(III) porphyrin geometry, have been used as described in the text.

Acknowledgment. The financial support of the State Committee for Scientific Research KBN (Grant 2 2651 92 03 to L.L.G.) and of the Centre National de la Recherche Scientifique (Grant URA 1194 to J.-C.M.) is kindly acknowledged.

IC9707927

(43) La Mar, G. N. In *NMR of Paramagnetic Molecules*; La Mar, G. N., Horrocks, W. D., Holm, R. H., Eds.; Academic Press: New York, 1974; pp 85−126.
(44) Balch, A. L.; Hart, R.; Latos-Grażyński, L.; Traylor, T. G. J. *Am. Chem. Soc.* **1990**, *112*, 7382.
(45) Morishima, I.; Yoshikawa, K.; Okada, K. *J. Am. Chem. Soc.* **1976**, *98*, 3787.
(46) Vaughan, J. D.; Mughrabi, Z.; Wu, E. C. *J. Org. Chem.* **1970**, *35*, 1141.